

## Variations of X-Ray Spectrum in Total Reflection X-Ray Fluorescence (TXRF) Analysis with Respect to Si Wafer Crystal Orientation for Different Incident Angles

Bor Wen Liou<sup>1</sup> and Chung Len Lee<sup>2</sup>

<sup>1</sup>*Department of Electrical Engineering, Wu-Feng Jr. College of Technology and Commerce, Chiayi, Taiwan 621, R.O.C.*

<sup>2</sup>*Department of Electronic Engineering and Institute of Electronics, National Chiao Tung University, Hsinchu, Taiwan 300, R.O.C.*

(Received May 11, 1999)

This work studies the W-L $\beta$ , Si-K, and spurious radiations, which occur in the total reflection X-ray fluorescence (TXRF) analysis technique. Measurements at different azimuth angles were studied with respect to the wafer orientation under different incident glancing angles of the X-ray beam on the surface of a bare Si-wafer, an oxide film, and an amorphous silicon film. It was found that both the W-L $\beta$  radiation and the spurious radiation signals have a four fold periodic variation with respect to the wafer orientation while the Si-K, radiation signal does not have such a variation. For the oxide wafers, this periodic variation for the W-L $\beta$  radiation and the spurious radiation signals becomes less and eventually disappears as the thickness of the oxide increases to 42 nm. For the amorphous silicon wafer, the above periodic variation phenomenon does not exist. This reveals that the W-L $\beta$  and the spurious radiation signals are mainly due to the interaction of incident X-ray evanescent radiation with the silicon crystal lattice. To reduce spurious signals in the TXRF analysis, a measurement at azimuth angle along the [100] directions of 45, 135, 225 or 315 degrees to the oxide-covered surface is suggested.

PACS. 63.20.Kr - Phonon-electron and phonon-phonon interactions.

PACS. 71.38.+i - Polarons and electron-phonon interactions.

### I. Introduction

Total reflection X-ray fluorescence (TXRF) spectrometry was introduced by Yoneda in 1971 [1] with the aim of improving the detection limits in energy-dispersive XRF (EDXRF) measurements, used for trace element analysis. It is used as an analyzing tool to monitor the surface cleanness of semiconductor wafers. The basic reason why TXRF is particularly suitable for surfaces is because of the low penetration depth of X-rays in the total reflection regime. This is an advantage when compared with EDXRF analytical methods, which use secondary radiation to restrict the penetration depth of the X-ray beam. TXRF keeps the secondary radiation comparatively unaffected by inelastic scattering, which contributes to the background signal. Therefore, TXRF analysis has a better detection limit, compared

to EDXRF analysis [2]. Although a low detection limit is a necessary condition for the majority of applications in trace element analysis, a straight TXRF without chemical pre-concentration is not sufficient in practice. Therefore, much work has been devoted to the development of tools to increase detection sensitivity, for example, in the vapor phase decomposition (VPD) method of sample preparation [3], and special software has been developed for calibration procedures [4].

The TXRF spectrum from a silicon wafer consists of two main peaks, which correspond to Si-K, and W-L, radiation, located at 1.74 KeV and 9.68 KeV, respectively. However, the intensity of the W- $L_{\beta}$  radiation varies widely with the azimuth angles of the measurement under the same X-ray beam incident angle [5, 6]. This intensity change has been attributed to Bragg reflection of the X-ray beam penetrating into the silicon wafer. This effect creates spurious signals [6]. Furthermore, Fe-K, and Ni-K, radiations appear when the intensity of the W- $L_{\beta}$  radiation is especially high [5, 6].

In this paper, variations in the TXRF X-ray spectrum in terms of the different measurement angles and the different X-ray beam incident angles on the silicon surface are studied in detail. The study covers not only incidence of the X-ray beam on the surface of bare silicon, but also on the surface of an oxide layer of various thicknesses and an amorphous silicon surface, which was deposited on the silicon wafer. It was found that the spurious Fe signal increased with the W- $L_{\beta}$  intensity, which is a function of the measurement azimuth angle of the crystal and the incident glancing angle of the X-ray excitation. For TXRF on the oxidized wafers, both the spurious Fe signal and the W-L, intensity decrease with an increase of the oxide thickness. For the amorphous silicon surface, they disappear, leading to the conclusion that they do come from the interaction between the evanescent wave of the incident X-ray with the lattice of the silicon surface. To reduce spurious signals, the best azimuth angles for a (110) wafer for TRXF measurements are 45, 135, 225, and 315 degrees. These findings can be useful in practical TXRF applications to the measurement of the trace metal impurities on a silicon wafer surface.

## II. Experimental procedure

The measurements were made by using an Atomika 8010 TXRF instrument, for which the X-ray source was a conventional W anode operated at 30 K and 65 mA. The radiation was a W- $L_{\beta}$  ray and the glancing incident angle of the X-ray beam was varied between 1 mrad and 2.5 mrad, which were below the critical incident angle of 3.2 mrad for the silicon wafer surface [4]. A Si(Li) solid state detector (SSD) with a Be window was used for detecting the fluorescence radiation of the sample. The analyzed area was 8 mm in diameter as defined by the detector aperture. The detector was cooled with liquid nitrogen and was mounted a few millimeters above the wafer surface. The measurement time was set to be 1000 seconds. The wafers used for analysis were boron-doped, (001) orientation, 8 inch wafers with a resistivity of 2.5 ~ 3.2 R-cm. Both the silicon dioxide layer and the amorphous silicon layer were grown on the surface of those wafers. The oxide thickness varied from 7.2 nm to 47.2 nm while the amorphous silicon thickness was 53.2 nm. To detect the metallic contamination of the above samples, inductively coupled plasma mass spectrometry (ICP-MS) measurements were also applied in conjunction with this TXRF method to double-check the results. Concerning spurious Fe signals in the

TXRF measurement, no Fe impurity on the surface of the bare silicon wafer was found by the ICP-MS method which used the cold plasma analysis [9].

### III. Results and discussion

#### III-1. Variation of X-ray spectrum on the surface of bare-silicon wafer

Fig. 1 shows the definition of the measurement angle of the X-ray beam with respect to the (110) orientation of the wafer. Fig. 2 shows the TXRF spectra at several measurement angles: 0, 22.5 and 45 degrees, under the X-ray beam incident angle of 2.5 mrad. The measurement position was at the center, which has the wafer coordinate (0,0). It can be seen that with an increase in the measurement angle, the intensity of the spectra generally decreases. The peaks at the lower energy (1.74 KeV) are identified to be the Si-K $_{\alpha}$  line and those at the higher energy (9.68 KeV) are the W-L $_{\beta}$  line. Four other peaks identified as corresponding to the impurity peaks of the Fe-K, line, the Co-K, line, the Ni-K, line and the escape (Cu) line, were also observed [10,11]. For all of these impurity peaks, those at the measurement angle of 0 degrees were the largest, those at the angle of 22.5 degree were the second largest and those at the 45 degree angle were the smallest. However, for this wafer, the VPD-ICP-MS analysis indicated no metallic impurity residues on the surface. These X-ray fluorescence peaks were "spurious peaks", which has been previously reported [5].

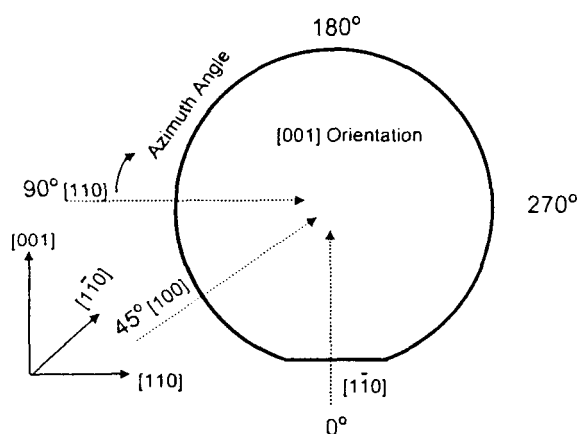


FIG. 1. Schematic picture of a silicon wafer with the definition of the measurement azimuth angle, the incident glancing angle of the X-ray beam and the crystallographic direction.

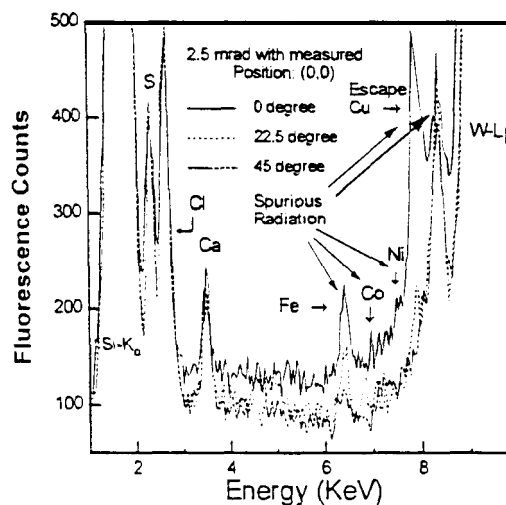


FIG. 2. A typical TXRF spectra obtained for three different measurement azimuth angles along the [100] direction, i.e., 0, 22.5 and 45 degrees at the center of the wafer for 2.5 mrad incident X-ray angle.

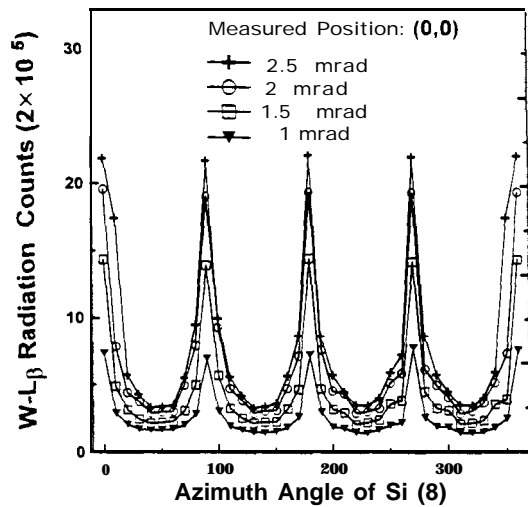


FIG. 3. The intensity counts of the  $W-L_{\beta}$  radiation in terms of the different measurement azimuth angles for four different incident angles, i.e., 2.5, 2.0, 1.5 and 1 mrad of the X-ray beam. The radiation shows a periodic variation with the measurement azimuth angle.

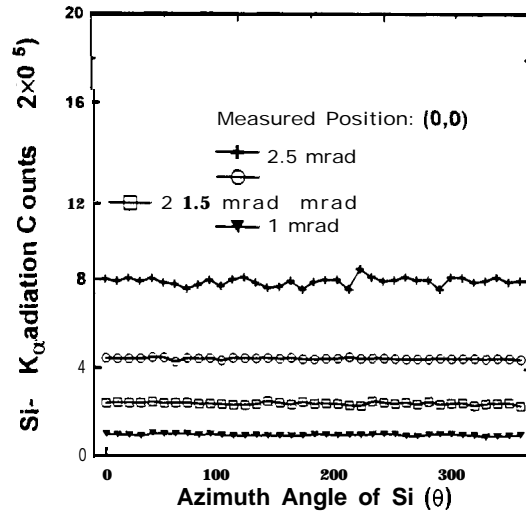


FIG. 4. The intensity counts of the  $Si-K_{\alpha}$  radiation in terms of the different, measurement azimuth angles for the same four incident angles of the X-ray beam. The radiation shows no variation with respect to measurement azimuth angle.

In order to investigate the spurious peaks with respect to the measurement azimuth angle and the X-ray beam incident angle, the evanescent  $W-L_{\beta}$  line and the fluorescent  $Si-K_{\alpha}$  line radiation were first measured with different measurement azimuth angles for several incident glancing angles. Fig. 3 and Fig. 4 show the  $W-L_{\beta}$  line and the  $Si-K_{\alpha}$  line radiation intensity plots, respectively. The  $W-L_{\beta}$  line radiation shows a strong dependence on the measurement azimuth angle, while the  $Si-K_{\alpha}$  line has only a weak dependence. For both lines, the larger the incident angle, the higher the intensity. The  $W-L_{\beta}$  line varies periodically with a period of 90 degrees with respect to the azimuth angle, i.e., the orientation of the wafer, where the 0, 90 e.t.c. degrees have the largest intensity and 45, 135 e.t.c. degrees have the lowest intensity. The 0, 90 e.t.c. degrees corresponded to the crystal orientation of the  $[110]$  planes and the 45, 135 e.t.c. degrees corresponded to the  $[100]$  planes. The (224) and (444) Bragg reflections of the evanescent beam penetrate into the Si wafer even under total external reflection conditions. Such an enhancement of the intensity is also expected for the  $\langle 110 \rangle$  azimuth [5, 6]. On the other hand, for the  $\langle 100 \rangle$  azimuth, the intensity is not enhanced because there is no lattice plane to satisfy the Bragg reflection condition [5, 6]. This periodic variation indicates that the  $W-L_{\beta}$  line radiation is a result of the interaction of the incident evanescent X-ray with the crystalline lattice of the substrate. The peaks of the spectrums are the cases where the Bragg condition

is satisfied [12]. The larger the incident angle, the higher the intensity. This is because more evanescent X-rays penetrate into the substrate and interact more with the crystalline lattice.

The spurious radiation peaks were also measured as a function of the measurement azimuth angle. One of the measured spurious signals, which corresponds to the Fe impurity, is plotted in Fig. 5 for several incident X-ray glancing angles. They also show a similar periodic variation with respect to the azimuth angle. The larger the incident X-ray angle, the higher the intensity. In fact, the spurious signal intensities are related to the intensity of the W-L $\beta$  line. Fig. 6 depicts plots of the total spurious counts with respect to the W-L $\beta$  counts for the four incident angles. All of the plots show that the intensity of the spurious radiations increases with the W-L $\beta$  line intensity. This close relationship of the spurious radiation with the W-L $\beta$  radiation leads to the suspicion that the spurious radiations come from the W-L $\beta$  radiation. It has been reported that the Fe signal can be excited by the W-L $\beta$  radiation in the solid state detector due to impurities at the Be window [13]. Hence, it is possible that the spurious signals at the Be solid state detector came from the W-L $\beta$  radiation.

From the above result, it can be concluded that, in order to reduce the spurious signals which blur the TXRF analysis result of metallic contamination, the incident measurement azimuth angle should be in the azimuthal angle along the [100] direction of 45, 135, 225 and 315 degrees.

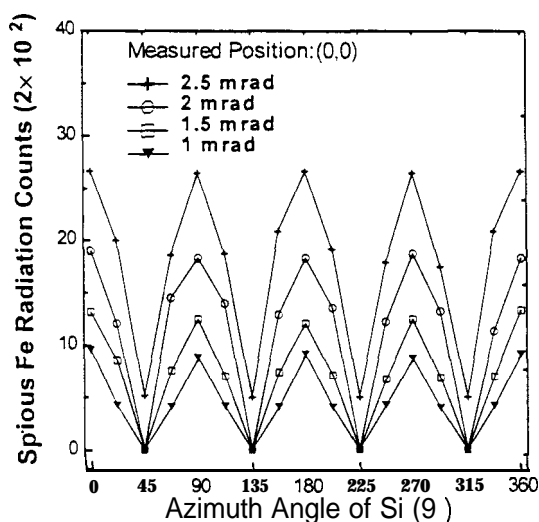


FIG. 5. The spurious Fe radiation counts in terms of the different measurement azimuth angles for the four different incident angles of the X-ray beam. It shows a periodic variation with the measurement azimuth angle.

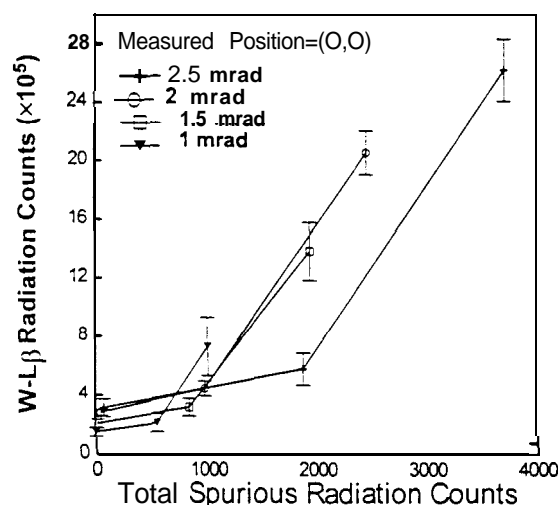


FIG. 6. The total spurious radiation counts versus the intensity of the W-L $\beta$  radiation.

### III-2. Variation of X-ray spectra on the surface of a silicon wafer with oxide or amorphous silicon layers

It is interesting to investigate TXRF spectra when the X-rays are incident on surfaces other than the bare silicon single crystal surface. Hence, the X-ray spectra of the TXRF incident on the surfaces of oxide layers of various thicknesses and on the surface of amorphous silicon were measured.

For this measurement, the incident beam of the X-ray was adjusted to be at a glancing incident angle far below the critical incident angle for the highest signal to noise ratio. Fig. 7 shows the Si-K $\alpha$  radiation fluorescence plots with respect to the X-ray incident angle for several surfaces with oxides and with the amorphous silicon film, respectively. The measurement time was set to be 20 sec for each measured point. For these samples, the oxides were grown at a temperature of 1000°C with dry O<sub>2</sub> growth while the amorphous silicon was deposited at 550°C. For the oxide surfaces, the larger the thickness, the smaller the applied critical angle. For an amorphous silicon surface, we applied a smaller critical angle, compared with the bare silicon single crystal surface. However, the background noise signal increased with the increasing incident glancing angle [8] and the surface with the thickest oxide, i.e., the 42.2 nm sample, showed the largest background noise intensity among all the samples for an X-ray incident beam of the 2 mrad incident angle.

Fig. 8 shows the intensity counts of the W-L $\beta$  radiation for the above samples. The incident angle of the X-ray beam was 2 mrad. It can be seen that the W-L $\beta$  radiation exhibited a periodic variation with respect to the measurement azimuth angle for the 2.5,

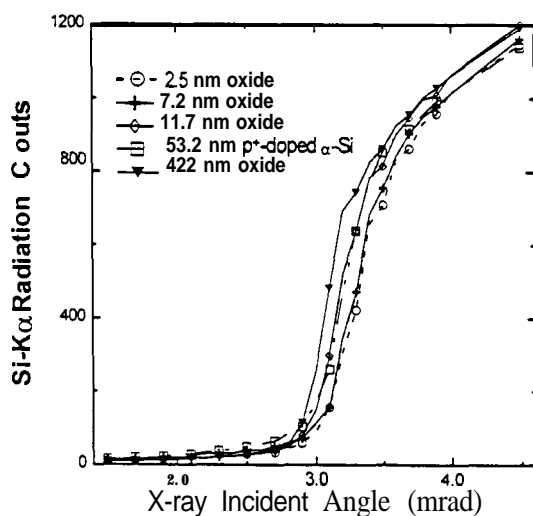


**FIG. 7.** The Si-K $\alpha$  radiation counts versus the X-ray incident angle for the oxides of different thicknesses and the amorphous silicon film.

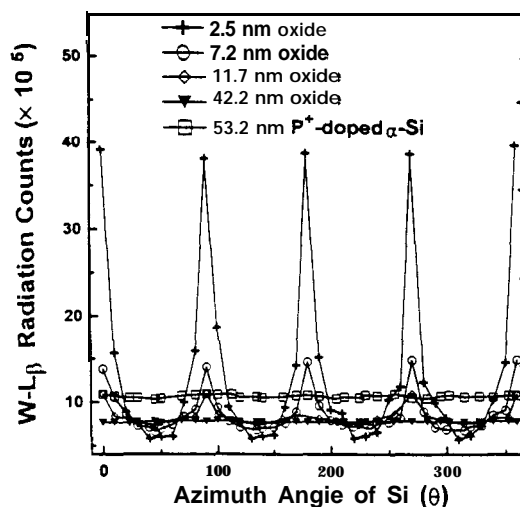


**FIG. 8.** The intensity counts of the W-L $\beta$  radiation in terms of the different measurement azimuth angles for the oxides of different thicknesses and the amorphous silicon film. The incident angle of the X-ray beam was 2 mrad.

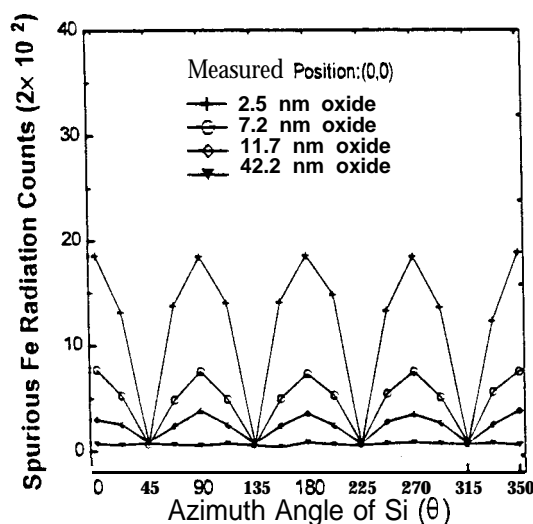


FIG. 9. The spurious Fe radiation counts in terms of the different measurement azimuth angles for the oxides of different thicknesses. The incident angle of the X-ray beam was 2 mrad.

7.2, and 11.7 nm oxide samples: the thicker the oxide, the smaller the periodic peak of the radiation. When the thickness of the oxide was increased to 42.2 nm, the periodic phenomenon disappeared. For the amorphous silicon sample: the periodic variation did not appear at all. This provided further evidence that the  $W-L_{\beta}$  radiation was a result of the interaction between the incident X-ray with the substrate crystal lattice.

Similarly, spurious signals corresponding to an Fe impurity were measured for samples with oxides of different thicknesses. Fig. 9 shows the measured signals for different measurement azimuth angles with an incident X-ray beam of 2 mrad incident angle. The signal has a periodic variation for the 2.5 nm oxide sample and the variation decreases as the oxide thickness increases. For the 42.2 nm oxide sample, the variation disappeared. This trend is the same as that of the W-L<sub>β</sub> radiation. This is a further indication that the spurious refraction signals are directly related to the W-L<sub>β</sub> radiation, which is a result of the interaction of the incident X-ray with the substrate crystal lattice.

Our results suggest that in order to minimize the spurious signal during the TXRF analysis, either the measurement azimuth angle along the [100] direction must be chosen to be at 45, 135, 225 or 315 degrees or the surface of the measured wafer must be covered with an oxide with a thickness greater than 42 nm.

#### IV. Conclusions

We reported on the W-L<sub>β</sub>, Si-K, and spurious radiations, which occur in the TXRF analysis technique. These spurious radiations can lead to erroneous results in identifying and determining metallic contamination. Our study has been in terms of different measurement azimuth angles with respect to the wafer orientation under different X-ray beam

incident glancing angles on the surface of bare Si-wafers, oxide film and amorphous silicon film. It was found that the  $W-L_{\beta}$  radiation and the spurious radiation signals have a four fold periodic variation with respect to the wafer orientation while the Si-K, radiation signal does not have such a variation. For the oxide wafers, this periodic variation in the intensity of the W-L, radiation and the spurious radiation signals becomes less and eventually disappears as the thickness of the oxide increases to 42 nm. For the amorphous silicon wafer, the above periodic variation phenomenon does not exist. This indicates that the W-L, and the spurious radiation signals are mainly due to the interaction of the evanescent radiation of the incident X-ray with the silicon crystal lattice. Also, from this study, it is suggested that, to reduce the spurious signals in the TXRF analysis, a measurement azimuth angle along the [100] direction of 45, 135, 225 or 315 degree on the oxide-covered surface should be used.

#### Acknowledgments

The authors would like to acknowledge the financial support of the National Science Council of the R.O.C. through the contract NSC-83-0404-E009-017 and the help of the Vanguard International Semiconductor Corporation.

#### References

- [1] Y. Yoneda and T. Horiuchi, *Rev. Sci. Instrum.* 42, 1069 (1971).
- [2] H. Schwenke, J. Knoth and U. Weisbrod, *X-ray Spectrometry*, 20, 277 (1991).
- [3] N. Streckfubss et al., *Fresenius J. Anal. Chem.* 343, 765 (1992).
- [4] W. Berneike et al., *Spectrochimica Acta*, 48B, 269 (1993).
- [5] K. Yakushiji et al., *Jpn. J. Appl. Phys.* 31, 2872 (1992).
- [6] K. Yakushiji et al., *Jpn. J. Appl. Phys.*, 32, 1191 (1993).
- [7] V. Penka and W. Hub, *Spectrochimica Acta*, 44B, 483 (1989).
- [8] P. Kregsamer, *Spectrochimica Acta*, 46B, 1333 (1991).
- [9] S. D. Tanner et al., *Atomic Spectroscopy*, 16, (1995).
- [10] L. Fabry et al., *Fresenius J. Anal. Chem.* 349, 439 (1994).
- [11] C. Strelt, H. Aiginger and P. Wobrauschek, *Spectrochimica Acta*, 44B, 491 (1989).
- [12] C. Kittel, *Introduction to Solid State Physics*, 6nd ed. (Wiley Student Edition, Singapore, 1986).
- [13] K. Yakushiji et al., *Jpn. J. Appl. Phys.*, Part 1, 33, 1130 (1994).